Sensors & Diagnostics

PAPER

View Article Online
View Journal | View Issue

Cite this: *Sens. Diagn.*, 2023, **2**, 347

A sensitive non-enzymatic electrochemical glucose sensor based on a ZnO/Co_3O_4/reduced graphene oxide nanocomposite†

Beshir A. Hussein, *[a] Abebaw A. Tsegaye,[b] Getabalew Shifera[c] and Abi M. Taddesse[d]

A novel sensitive and selective ZnO/Co_3O_4/rGO nanocomposite was fabricated using a hydrothermal method and used as a non-enzymatic electrochemical sensor for the detection of glucose. The morphology and structure of the ZnO/Co_3O_4/rGO composite were characterized using UV-vis spectroscopy, X-ray diffraction (XRD) and Fourier transform infrared (FTIR) techniques. The electrochemical properties of the as-synthesized nanomaterials were characterized by cyclic voltammetry (CV), electrochemical impedance spectroscopy (EIS), and single potential time base (TB) amperometry. The ZnO/Co_3O_4/rGO nanocomposite exhibited excellent electrochemical performance with higher catalytic activity, lower working potential (0.55 V), and low charge transfer resistance for the electrochemical oxidation of glucose, which can be attributed to the presence of high conductive reduced graphene oxide sheets on the surface of the electrode. Under optimal conditions, the ZnO/Co_3O_4/rGO glassy carbon electrode (GCE) modified electrochemical glucose sensor demonstrated a wide linear range (0.015–10 mM), high sensitivity (1551.38 μA mM^{-1} cm^{-2}), low detection limit (0.043 μM) and fast response time (~3 s) to glucose determination. In addition, the ZnO/Co_3O_4/rGO/GCE sensor was able to detect glucose even in the presence of biologically interfering molecules and chloride ions. The sensor achieved appreciable repeatability, reproducibility, and long-term stability. Moreover, the practical application of the ZnO/Co_3O_4/rGO/GCE electrochemical sensor is very appropriate for the detection of glucose in real samples for medical diagnostic and food industries, and the results positively agreed with those collected using the spectrophotometric method in the hospital and the glucose label value in food industries.

Received 17th October 2022,
Accepted 2nd December 2022

DOI: 10.1039/d2sd00183g

rsc.li/sensors

1. Introduction

Diabetes is a group of metabolic diseases affecting about 150 million people worldwide, and it is one of the leading causes of death and disability, such as blindness, nerve degeneration, and kidney failure.[1,2] This metabolic disorder results from insulin deficiency and hyperglycaemia and it is reflected by blood glucose concentrations higher than the normal range of 80–120 mg dL^{-1} (4.4–6.6 mM).[3] According to the World Health Organization (WHO) and the International Diabetes Federation (IDF), its worldwide prevalence is projected to double over the next couple of decades, from 347 million people in 2005 to 700 million people in 2030.[4,5] Notably, greater than 80% of patients with diabetic live in low and middle-income countries.[4]

Glucose concentration acts as a crucial indicator in diseases such as diabetes and endocrine metabolic disorders. The development of reliable and rapid methods for glucose monitoring is important in many areas such as clinical diagnostics, biotechnology, and food industries.[6] Therefore, it is of significant importance to developing fast, accurate, and stable technologies to detect glucose levels and frequent testing of physiological blood glucose levels to avoid diabetic emergencies.[5,7]

However, it is difficult to detect it by conventional photometric technologies because glucose lacks chromophoric and fluorophoric ligands.[8] In industry and laboratory-based testing, the HPLC system can be used to separate different sugars and alcohols prior to oxidation at the non-enzymatic electrode, thus avoiding the issue of interferences. This is not possible for blood glucose sensors because chromatographic systems are not practical in terms of self-testing using *in vitro* handheld glucose meters, and

[a] *Department of Chemistry, Mekdela Amba University, P.O. BOX 32, Mekane Selam, Ethiopia. E-mail: beshir45@gmail.com*
[b] *Department of Chemistry, Bahir Dar University, P.O. BOX 79, Bahir Dar, Ethiopia*
[c] *Department of Chemistry, Mettu University, P.O. BOX 318, Mettu, Ethiopia*
[d] *Department of Chemistry, Haramaya University, P.O. BOX 138, Dire Dawa, Ethiopia*

† Electronic supplementary information (ESI) available. See DOI: https://doi.org/10.1039/d2sd00183g

they are certainly incompatible with *in vivo* analysis[9] and it requires many steps while consuming time, reagents, and samples.[10] Due to the simplicity of the instrumentation and operation, electrochemical detection has become popular.[8]

Electrochemical glucose sensors generally fall into two categories, namely, enzymatic and nonenzymatic. However the enzymatic glucose sensors (glucose dehydrogenase and glucose oxidase) have dominated the market, and they suffer from various drawbacks that originate from the inherent instability of the enzymes. These difficulties can be overcome by the use of highly improved, sensitive, and selective non-enzymatic glucose sensors.[11]

A tremendous amount of non-enzymatic glucose (NEG) sensor research is ongoing all around the world, as evidenced by the exponential increase in the number of publications over recent years.[12] However, high-cost noble metals (Pt, Ag, and Au) also proved to be extremely non-selective and susceptible to poisoning by various components of blood and adsorbed chloride ions.[13] Therefore, increasing attention has been focused on fabricating high-performance enzyme-free devices using inexpensive and resourceful transition-metal oxide catalysts such as Cu_2O,[14] CuO,[15] MnO_2,[16] ZnO,[7] CuO,[1] ZnO/CuO,[17] Co_3O_4/NiO,[18] NiO/CuO/rGO,[19] NiO/Au/PANI/RGO,[20] due to their high electrocatalytic activity and high anti-poisoning resistance toward intermediate compounds and chloride ions.

Cobalt and cobalt oxide NPs have been widely used in nonenzymatic amino acid sensors but rarely reported for glucose detection because pure Co_3O_4 NPs could form severe particle aggregation structures after they are assembled on an electrode, which will reduce their specific surface area and hinder the mass transfer.[6] The nanostructured ZnO also shows high sensitivity but very poor stability because the ZnO nanostructure is easily removed from the electrode surface during functionalization.[21] Indeed, improved stability without the loss of sensitivity or selectivity is one of the big challenges for glucose monitoring.[5] The drawback of the intrinsic poor conductivity of cobalt oxides, the hierarchical growth or combination of cobalt oxides on carbonaceous substrates *e.g.*, graphene, reduced graphene oxide (rGO), and carbon nanotubes (CNTs) have been proven to be a popular strategy to improve their electron transport capability and also to avoid the severe aggregation of cobalt oxide.[22]

Graphene, graphene oxide (GO) and reduced graphene oxide (rGO) when mixed with metal oxides produce potential composite materials with great promise for the large-scale production of selective chemical and biosensors for cost-effective applications in the areas of environmental pollution, safety, and security, and clinical and pharmacological analysis.[23,24] However, studies on the use of Co_3O_4 and ZnO nanoparticles and their composites with rGO towards NEG sensors have not been reported so far.

There are various growth processes to produce metal oxide nanostructures on graphene sheets, such as *in situ* chemical synthesis,[24,25] hydrothermal processes,[26] microwave heating,[27] and electrodeposition.[28] In this work, the Co_3O_4 NPs and ZnO NPs were grown on the surface of graphene sheets using the hydrothermal method and could be used for nonenzymatic glucose sensing owing to their excellent catalytic activity toward electrochemical oxidation of glucose in NaOH electrolyte.

2. Materials and methods

2.1. Chemicals and reagents

β-Glucose ($C_6H_{12}O_6$), sodium hydroxide (NaOH), sodiumcarbonate (Na_2CO_3), cobalt nitrate ($Co(NO_3)_2{\cdot}6H_2O$), maltose ($C_{12}H_{22}O_{11}$), fructose ($C_6H_{12}O_6$) and sucrose ($C_{12}H_{22}O_{11}$) were purchased from BDH chemicals. Zinc nitrate hexahydrate ($Zn(NO_3)_2{\cdot}6H_2O$), oxalic acid ($H_2C_2O_4{\cdot}2H_2O$), ascorbic acid ($C_6H_8O_6$), and uric acid ($C_5H_4N_4O_3$) were obtained from Blulux Laboratories, whereas reduced graphene oxide (rGO) was purchased from Medreich chemicals.

2.2. Synthesis of Co_3O_4 nanoparticles

Cobalt oxide nanoparticles were synthesized by the simple precipitation method by modification of the previous report.[29] A solution of 0.2 M hexahydrate cobalt nitrate (14.55 grams in 250 ml) and 0.2 M oxalic acid (6.3 grams in 250 ml) were prepared separately in deionized water and continuous stirring was performed for 1 hour and 30 minutes, respectively. Oxalic acid ($H_2C_2O_4$) was then mixed into the metal salt solution dropwise with continuous stirring for three hours. The resultant light pink coloured cobalt oxalate precipitate (CoC_2O_4) was thus obtained. The precipitate resulting from the reaction between the two solutions was allowed to settle for 1 h, filtered with Whatman filter paper, washed three times with deionized water and ethanol, and then dried at 80 °C in the oven for 6 hours. Finally, the precursor thus obtained, after drying was decomposed at 600 °C for 2 hours in a muffle furnace to obtain black colour Co_3O_4 nanoparticles.

2.3. Synthesis of ZnO nanoparticle

ZnO NPs were prepared by a precipitation method according to a previous report.[30] Zinc nitrate hexahydrate ($Zn(NO_3)_2{\cdot}6H_2O$) and sodium carbonate (Na_2CO_3) solutions were separately prepared by dissolving 29.747 g of $Zn(NO_3)_2{\cdot}6H_2O$ in 200 ml deionized water (0.1 mol) and 12.7188 g of Na_2CO_3 in 240 mL of deionized water (0.12 mol). $Zn(NO_3)_2{\cdot}6H_2O$ solution was slowly dripped into Na_2CO_3 solution and the mixture was stirred continuously for 2 h. The white precipitate resulting from the reaction between the two solutions was allowed to settle for 24 h and filtered using Whatman filter paper and washed three times with deionized water and ethanol. The filtered/washed precipitate was dried at 100 °C for 6 h to form the precursor for ZnO. The precursor was thus obtained, after drying and calcined at 300 °C for 2 h in a muffle furnace to obtain nano-ZnO particles.

2.4. Synthesis of ZnO/Co_3O_4 nanocomposite

In a typical synthesis process of ZnO/Co_3O_4 natfgap nitrate hexahydrate [$Zn(NO_3)_2{\cdot}6H_2O$] and 1.8 M sodium hydroxide (NaOH) were prepared in separated beakers by dissolving 40.1 g of [$Zn(NO_3)_2{\cdot}6H_2O$] and 10.8 g of NaOH in 150 ml of distilled water. Then, the beaker containing NaOH solution was heated at a temperature of about 55 °C. The [$Zn(NO_3)_2{\cdot}6H_2O$] solution was added dropwise (slowly for 1.5 h) to the above-heated solution under high-speed stirring.[10] In the obtained milky solution, 2 g of synthesized Co_3O_4 nanoparticles were added. The beaker was sealed under these conditions for 2 h. The precipitate was washed with deionized water and ethanol and then dried at 60 °C for 6 h. The dry sample was annealed in a muffle furnace at 300 °C for 2 h when the gray-colored ZnO/Co_3O_4 nanocomposite was formed.

2.5. Synthesis of ZnO/Co_3O_4/rGO nanocomposite

A facile and environment-friendly strategy was first proposed in this work to prepare ZnO/Co_3O_4/rGO nanocomposite in ethanol solution without the addition of toxic solvents (Scheme 1). This method allows for the growth of nanoparticles on graphene without the need for post-annealing and calcination. In a typical experiment, 5 mg rGO was dispersed in 60 mL ethanol and sonicated for 2 h and in another beaker 6.3 g of synthesized ZnO/Co_3O_4 nanocomposite was dissolved in 100 ml of deionized water, and then stirred for 2 h at the temperature of 55 °C to obtain a homogenous suspension. Then, the reduced graphene oxide solution was added into the ZnO/Co_3O_4 nanocomposite solution in a dropwise manner with stirring under a nitrogen atmosphere and the temperature was adjusted at room temperature. The resultant suspension was separated using centrifugation and thoroughly washed with deionised water and ethanol to remove impurities and dried overnight at 80 °C to yield ZnO/Co_3O_4/rGO ternary nanocomposite.[31,32] The growth mechanism of ZnO and Co_3O_4 nanostructures on graphene is due to the attraction of positively-charged metal/metal-oxide ions by the polarized bonds of the functional groups on the graphene (such as –OH, C═O of carboxylic, O═C–O of carboxylate, C–O and O–C–O).[33]

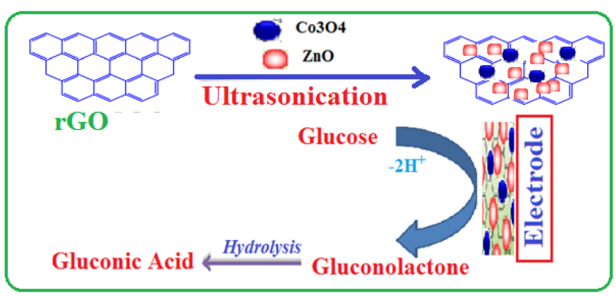

Scheme 1 Schematic illustration for the fabrication of ZnO/Co_3O_4/rGO/GCE-modified electrode and its mechanism for amperometric detection of glucose.

2.6. Characterization of nanomaterials

The phase structure of as-prepared modifiers was recorded using X-ray diffraction (XRD; BRUKER D8, AXS GmbH, Karlsruhe, Germany). For structural characterization, Fourier transform infrared (FTIR) spectra (KBr pellets) were recorded using an SP65 instrument (PerkinElmer), and UV-vis absorption spectra were recorded using a UV-vis spectrophotometer (SANYO, SP65). A scanning electron microscope (SEM; JEOL JSM848) was used to study the morphology of the as-synthesized materials.

2.7. Preparation of modified glass carbon electrode

First, the GCE surface was polished with 1.0, 0.3, and 0.05 μm alumina powder and then washed with deionized water, followed by sonication in ethanol and dried at room temperature to remove the adsorbed alumina slurry. The ZnO/Co_3O_4/rGO nanocomposite-modified GCE was fabricated by a simple drop coating method based on the previous report.[17] The as-prepared nanocomposite was dispersed in ethanol at about 5 mg mL^{-1} and then sonicated well to obtain a uniform suspension. Next, 8 μL suspension of ZnO/Co_3O_4/rGO was coated on bare GCE and the electrode was kept in the air oven at 35 °C until the film was completely dried. For the control modified electrodes such as ZnO/GCE, Co_3O_4/GCE, and ZnO/Co_3O_4/GCE were fabricated by the same experimental procedure.

2.8. Electrochemical studies

All electrochemical measurements were conducted using a BAS 100B (USA) electrochemical analyser controlled by the Windows software. Three electrode configurations were used throughout the experiments using modified GCE as the working electrode, a platinum wire as an auxiliary, and Ag/AgCl/(saturated KCl) as the reference electrode. All the cell potentials were measured with respect to Ag/AgCl/Cl^- reference using 0.1 M NaOH aqueous electrolyte. The electrochemical activity of the modified electrodes was evaluated using cyclic volumetric and electrochemical impedance spectroscopy in 0.1 m NaOH aqueous solution. Amperometric detection of glucose was carried out by continuously adding glucose under magnetic stirring with an applied potential of 0.55 V for various glucose concentrations in an electrochemical cell containing a magnetically stirred NaOH electrolyte.

3. Results and discussion

3.1. Structural and morphology characterization

Fig. 1 shows the UV-vis absorption spectra of pristine Co_3O_4 and ZnO, ZnO/Co_3O_4, and ZnO/Co_3O_4/rGO nanocomposites. The sharp characteristic absorption peak at 378 nm, corresponding to a band gap value of 3.28 eV, indicates the

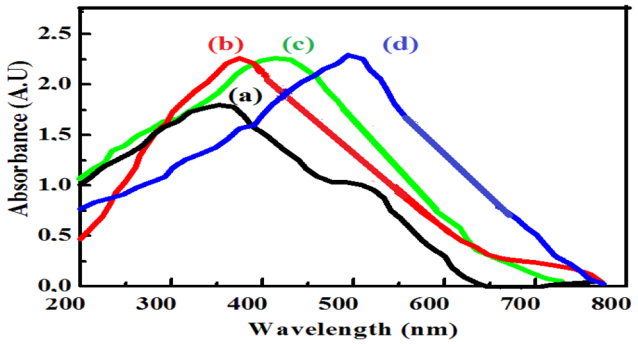

Fig. 1 UV-vis absorbance spectra of (a) Co_3O_4 NPs, (b), ZnO NPs, (c) ZnO/Co_3O_4 nanocomposite and (d) ZnO/Co_3O_4/rGO nanocomposite.

presence of ZnO nanostructures and it was agreed with other reports.[29] The Co_3O_4 nanoparticles have two broad peaks originating at around 358 nm and 520 nm (Fig. 1b), which are quite close to other reported Co_3O_4 systems.[18] The multiple band gaps of the Co_3O_4 nanoparticles are attributed to the possibilities of O^{2-} to Co^{2+} and O^{2-} to Co^{3+} charge transfer processes in the Co_3O_4 nanoparticles, as observed in the Co_3O_4 quantum dots in cubic morphology.[34] Intense absorption bands observed at around 406 nm for the ZnO/Co_3O_4 binary system (Fig. 1c) are due to the presence of Co_3O_4 nanoparticles. The ZnO/Co_3O_4/rGO ternary system, on the other hand, revealed a broad elevated background in the visible region, which is mainly due to rGO and intense absorbance in comparison to pure ZnO and Co_2O_3 nanoparticles (Fig. 1d) similar to that in other reports.[31] The presence of rGO is the cause of the red shift in the absorption maxima of the ternary nanocomposite.

Fig. 2 shows FTIR spectra of the as-synthesized nanomaterials recorded in the range of 4000–400 cm^{-1}. The broad bands in the range 3431–3684 cm^{-1} and 1630–1640 cm^{-1} could be attributed to O–H stretching and bending vibrations of the adsorbed H_2O molecules, respectively.[35]

The peak appearing at about 455 cm^{-1} is assigned to the zinc–oxygen (Zn–O) stretching mode.[36] The absorption band at 564 cm^{-1} was due to the Co–O stretching vibration mode and the band at 662 cm^{-1} is due to the bridging vibration of the O–Co–O bond and it is in good agreement with reported literature values.[36,37] The absorption bands at 2918 cm^{-1} indicated the aromatic C–H bond of reduced graphene oxide. The analysis above suggests that it is not a simple mix between ZnO/Co_3O_4 and rGO, but rather an interaction existing at the interfaces of ZnO/Co_3O_4 nanocomposite and reduced graphene oxide. No other peaks appear in the spectra, which confirmed the formation of pure ZnO/Co_3O_4/rGO nanocomposite.

Fig. 3 shows the XRD analysed data of the as-prepared Co_3O_4 NPs, ZnO NPs, Co_3O_4/ZnO, and ZnO/Co_3O_4/rGO nanocomposites. In the XRD pattern of the ZnO nanoparticles (Fig. 3), the diffraction peaks at scattering angles (2θ) around 31.77, 34.35, 36.27, 47.59, 56.57, 62.93, 67.89, and 69.2 correspond to (100), (002), (101), (012), (110), (013), (112) and (201) hexagonal crystalline planes of ZnO, respectively (JCPDS 962300113). The XRD pattern of the prepared Co_3O_4 NPs (Fig. 3) showed 2θ values of 19.06, 31.45, 36.95, 44.95, 59.46, and 65.49 corresponding to the crystal planes of (111), (202), (131), (040), (151) and (404) confirming the formation of pure cubic phase of Co_3O_4 NPs (JCPDS 961538532). All peaks confirmed the presence of both the hexagonal phase of zinc oxide and the cubic phase of Co_3O_4, which demonstrated the formation of ZnO and Co_3O_4 without impurities, and all the peaks of the final product matched either with Co_3O_4 or ZnO NPs. Thus, the same crystal phases of ZnO and Co_3O_4 were retained in both binary and ternary nanocomposites. However, in the ternary composite, the characteristic peak at 24.16 accounted for the (002) reflection of graphitic carbon, confirming the stacking

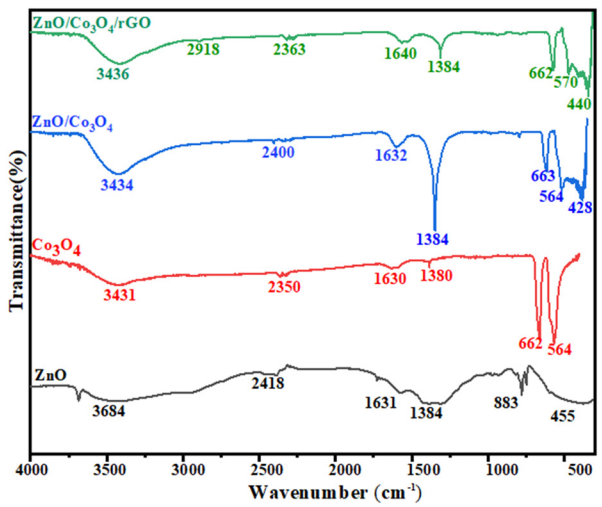

Fig. 2 FTIR spectrum of ZnO NPs, Co_3O_4 NPS, ZnO/Co_3O_4 nanocomposite, and ZnO/Co_3O_4/rGO nanocomposite.

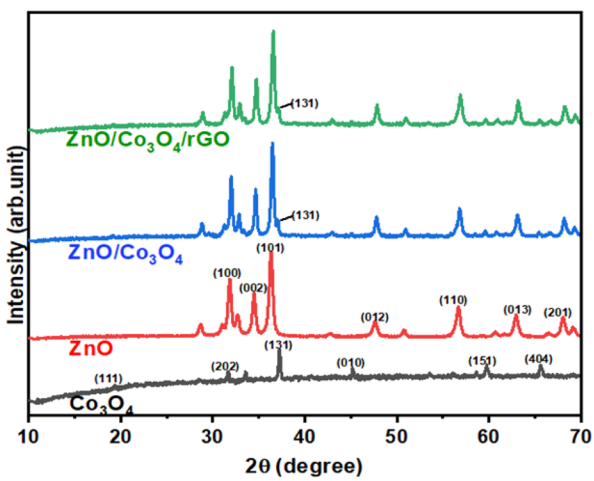

Fig. 3 XRD patterns of, Co_3O_4 NPs, ZnO NPs, ZnO/Co_3O_4 and ZnO/Co_3O_4/rGO nanocomposites.

structure of the rGO sheet, which is in good agreement with that from the literature.[38] The average particle size (D) of the synthesized sensors can be calculated using Scherer's formula.

$$D = \frac{K\lambda}{\beta \cos\theta} = \frac{0.90\lambda}{\beta \cos\theta}$$

where, K = 0.90 is the Scherrer's constant, λ is the X-ray wavelength, θ is Bragg's diffraction angle, 2θ is the angle between the incident and diffracted X-ray, and β is the peak width of the diffraction line at half of the maximum intensity. The average particle sizes of Co_3O_4 NPs, ZnO NPs, ZnO/Co_3O_4 and ZnO/Co_3O_4/rGO nanocomposites were 44.9, 21.9, 25.2 and 17.5 nm, respectively. The ternary ZnO/Co_3O_4/rGO nanocomposite showed the highest surface area as a result of the decreased particle size due to the synergistic effects between the components of ZnO, Co_3O_4, and rGO in the composite system.

The morphological SEM images of ZnO, Co_3O_4, ZnO/Co_3O_4, and ZnO/Co_3O_4/rGO are displayed in Fig. 4. As can be seen, pristine ZnO and Co_3O_4 nanoparticles, and ZnO/Co_3O_4, ZnO/Co_3O_4/RGO nanocomposites showed distinct morphologies. Foam-like irregular structures were observed for ZnO (Fig. 4a), while nanowires with spherical symmetry were observed for Co_3O_4 (Fig. 4b). Characteristic morphology of ZnO and Co_3O_4 appeared in the nanocomposite, small foam over plate-like morphology with different sizes was seen in the ZnO and Co_3O_4 nanocomposite (Fig. 4c), whereas this mixture grew over folded sheets of rGO, exfoliated as well as wrinkles rGO is indicated for the ternary system (Fig. 4d). The thickness of a single reduced rGO agreed with that from the other studies.[6]

3.2. Electrocatalytic oxidation of glucose

A comparative study of the electrocatalytic performance of different electrodes for glucose oxidation was conducted in 0.1 M NaOH aqueous solution in the presence and absence of glucose in a potential window of 0.0 to 0.8 V and at a scan rate of 50 mV s^{-1} using CV. Fig. 5 shows the cyclic voltammograms (CVs) of different electrodes in 0.1 M NaOH aqueous solution without glucose (i) and containing 2 mM glucose (ii). The voltammogram obtained at bare GCE (Fig. 5a) revealed that no noticeable redox behavior was observed and it indicating that the bare GCE was potentially inert under the alkaline medium,[18] while Co_3O_4/GCE, ZnO/GCE, ZnO/Co_3O_4/GCE and ZnO/Co_3O_4/rGO/GCE (Fig. 5b–e) displayed well-defined redox peaks. However, at the same scan rate, ZnO/Co_3O_4/GCE showed much larger peak currents (Fig. 5f) than that of single metal oxide-modified glass carbon electrodes. This result reveals that the electrochemical performance of the hybrid nanocomposites is greatly enhanced compared to its individual counterparts of metal oxide nanoparticles.[39]

As clearly shown in Fig. 5(f), the anodic peak current of the ZnO/Co_3O_4/rGO modified electrode was approximately 8 times, 7 times, and 2.5 times higher than that of Co_3O_4 NPs, ZnO NPs, Co_3O_4/ZnO nanocomposite modified electrodes, respectively, and exhibited outstanding electrochemical performance with higher catalytic activity and lower electrocatalytic potential (0.5 V) for glucose oxidation. The negative shift of the overpotential can be ascribed to a kinetic effect by an increase in the electroactive surface area and the electron transfer rate from glucose to the modified electrodes.[40]

The increase in the electrochemical performance was mainly attributed to the presence of rGO and good dispersion in ZnO/Co_3O_4 nanocomposite, which improved the electrical

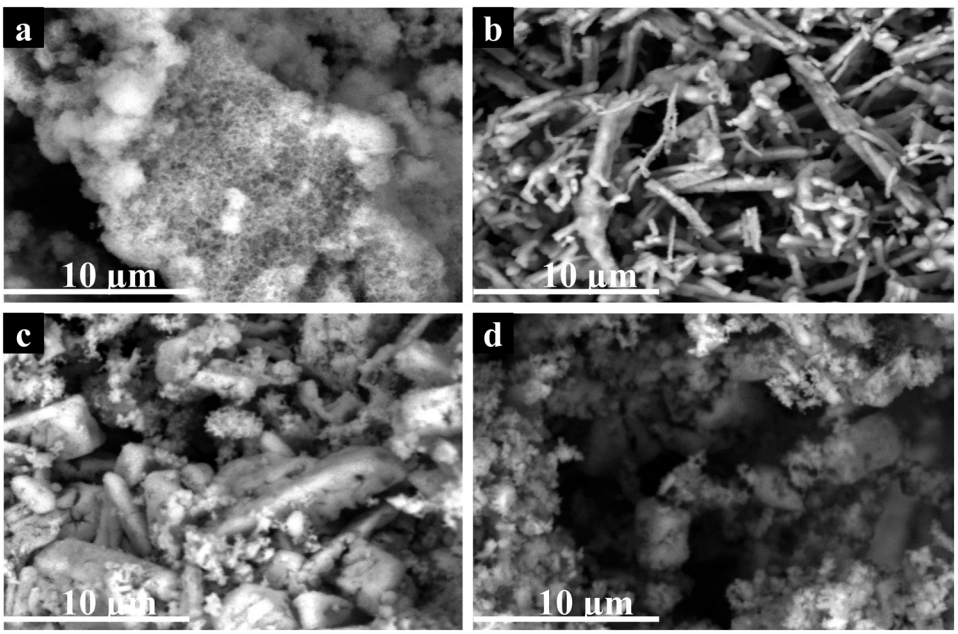

Fig. 4 SEM images of a) ZnO, b) Co_3O_4, c) ZnO/Co_3O_4, and d) ZnO/Co_3O_4/rGO.

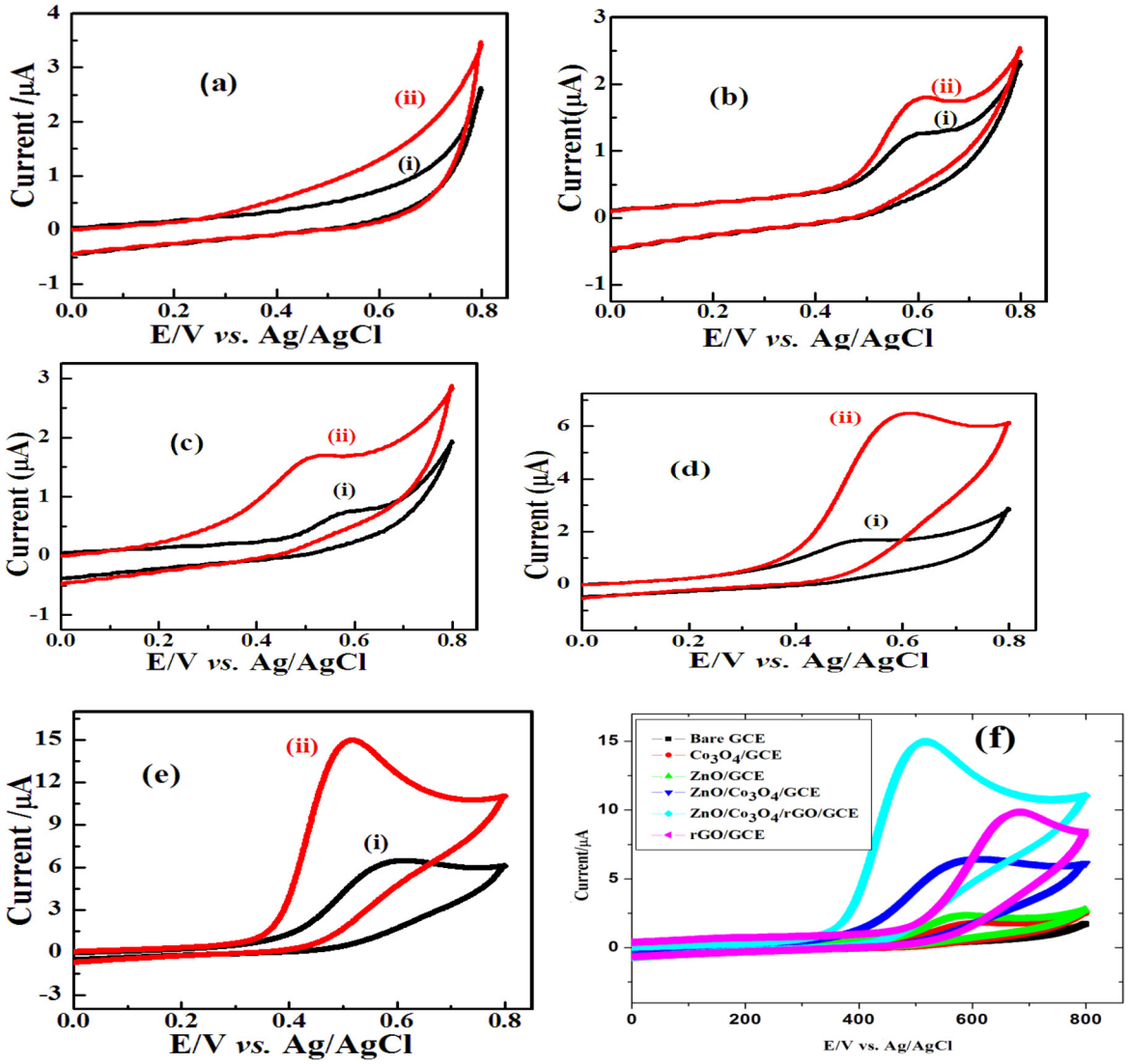

Fig. 5 CVs of (a) bare GCE, (b) Co_3O_4/GCE, (c) ZnO/GCE, (d) ZnO/Co_3O_4/GCE, (e) ZnO/Co_3O_4/rGO/GCE in the absence (i), presence (ii) of 2 mM glucose and (f) electrodes under study in the presence of 2 mM glucose in 0.1 M NaOH at a 50 mV s^{-1} scan rate.

conductivity of the composite and the electrochemical utilization of the pristine metal oxide nanocomposite during the electrochemical activity. The rGO also provided a large surface area to increase the quantity of the metal oxide nanoparticles and the large surface-to-volume ratio of the ZnO/Co_3O_4/rGO nanocomposites produced a large total surface area that provided more chances to contact glucose.

Ding *et al.*[41] and Ramasamy *et al.*[18] reported two sets of redox peaks for cobalt oxide-modified electrodes in 0.1 M NaOH supporting electrolyte. According to Mian *et al.*[42] and Gao *et al.*,[43] a pair of redox peaks Co(II)/Co(III) was seen in a low potential zone around 0.15 V (*vs.* Ag/AgCl), which indicates the reversible transition of Co_3O_4 into CoOOH. However, in this work, only one set of good redox peaks appeared at an anodic potential of 0.60 V (*vs.* Ag/AgCl) and the oxidation for glucose occurs only at the redox centre Co(III)/Co(IV). According to the previous report, the appearance of the Co(II)/Co(III) redox peaks possibly depends upon factors that come either from itself or outside, such as the electrolyte concentration, scan rate, and thickness of the active materials.[44] In the potential region above 0.45 V (*vs.* Ag/AgCl), the transition of Co(III) to Co(IV) is much stronger than that for the transition of Co(II) to Co(III), suggesting that the electro-oxidation of glucose is mainly mediated by the Co(III)/Co(IV) redox couple rather than the Co(II)/Co(III) redox couple for the Co_3O_4-based catalysts in an alkaline solution.[42] According to the above results and previous conclusions, the possible redox mechanism involving the electrochemical oxidation of glucose in NaOH solution could be described with the following equations.[6] The mechanism of the electrochemical oxidation of glucose catalyzed by Co_3O_4 nanoparticle-containing electrodes is proposed, in that Co_3O_4 was oxidized to CoOOH, and then CoOOH was further oxidized to CoO_2, which oxidized glucose to generate gluconolactone and CoOOH (eqn (1) and Scheme 1).

$$Co_3O_4 + OH^- + H_2O \rightarrow 3CoOOH + e \quad (1)$$

$$CoOOH + OH \rightarrow CoO_2 + H_2O + e \quad (2)$$

$$2CoO_2 + C_6H_{12}O_6 \text{ (glucose)} \rightarrow 2CoOOH + C_6H_{10}O_6 \text{ (gluconolactone)} + 2H^+ + 2e^- \quad (3)$$

3.3. Effect of scan rate on the electrochemical oxidation of glucose

The effect of scan rate on the oxidation of glucose in a 0.1 M NaOH solution in the presence of 2 mM glucose on the ZnO/Co_3O_4/rGO electrodes was investigated using cyclic voltammetry and the results are shown in Fig. 6. It was found that anodic and cathodic peak currents increase distinctly with the increasing potential scan rate in the range of 10–100 mV s^{-1}. When the peak current (i_{pa}) was plotted against the square root of scan rate ($v^{1/2}$), a linear relationship with regression equations I_{pa} (μA) = 0.887X + 0.616 (R^2 = 0.9965). These results indicate that electrochemical kinetics is a typical diffusion-controlled electrochemical process, which is ultimate for the detection of glucose.

3.4. Electrochemical impedance spectroscopy (EIS) studies

In order to investigate the electrochemical behavior of the modified electrodes, EIS analyses were performed in a solution containing 2 M glucose in 0.1 M NaOH at a scanning frequency range of 10–1000 Hz. The Nyquist plots indicated (Fig. 7) that the EIS spectra consisted of a semicircular portion (corresponds to the electron transfer limited process) and a linear portion corresponding to the diffusion-limited process.

The bare electrode showed a large semicircle compared to the other modified electrodes, which indicated a large charge-transfer resistance (R_{ct}) at the electrode/electrolyte interface due to the sluggish electron transfer kinetics. It can obviously be seen that R_{ct} decreased for the Co_3O_4/GCE (1450 ohms), ZnO/GCE (1245 ohm), ZnO/Co_3O_4/GCE (730 ohms), and ZnO/Co_3O_4/rGO/GCE (525 ohms) modified electrodes, which can be attributed to the presence of highly conductive rGO sheets on the electrode surface and it is a good electrocatalytic performance for the oxidation of glucose.

3.5. Optimization of experimental conditions

The influence of NaOH concentration was studied on amperometric measurements for detecting 2 mM glucose. An alkaline medium is required to enhance the electrocatalytic activity of transition metal electrodes toward the oxidation of carbohydrate compounds.[45] It can be seen that the peak currents of the CV graphs increased with changing the NaOH concentration from 0.005 M to 0.1 M. However, a further increase in NaOH concentration gave rise to a decrease in the peak currents of the CV graphs. Therefore, the concentration of sodium hydroxide for glucose detection by the developed electrode was chosen to be 0.1 M and a similar observation was also reported.[46]

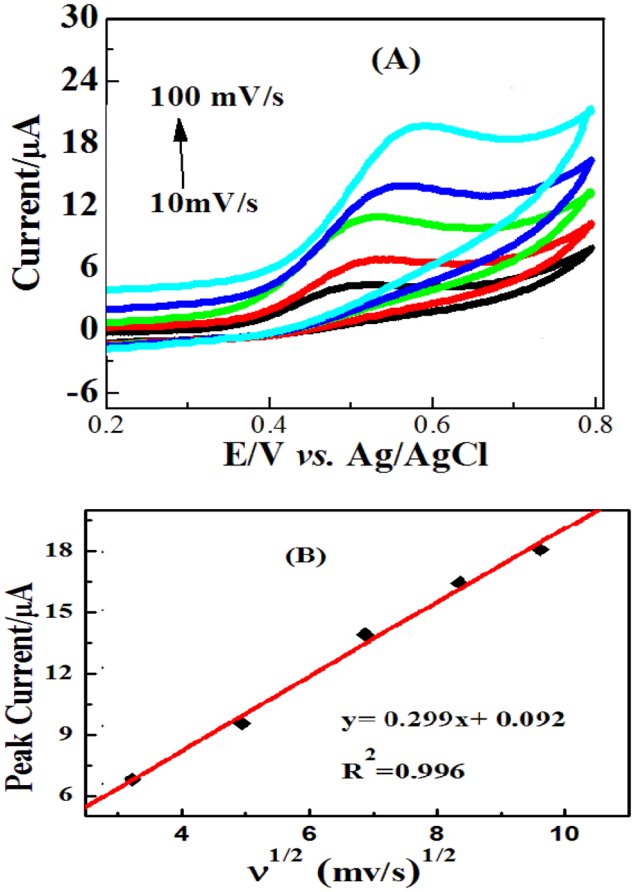

Fig. 6 (A) Effect of the scan rate (10–100 mV s^{-1}) on the cyclic voltammogram ZnO/Co_3O_4/rGO in the presence of 0.1 M NaOH and 2 mM glucose. (B) The plot of current against the square of the scan rate ($v^{1/2}$).

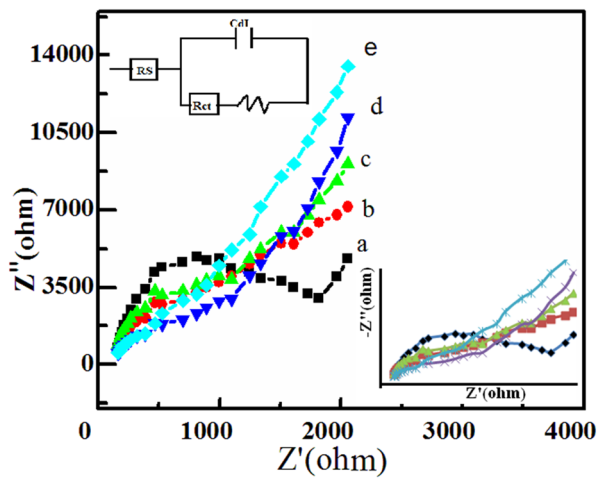

Fig. 7 EIS measurement of bare electrode (a), Co_3O_4/GCE (b), ZnO/GCE (c), ZnO/Co_3O_4/GCE (d) and ZnO/Co_3O_4/rGO/GCE (e) in 0.1 M NaOH solution containing 2 mM glucose. The inset circuit is the equivalent circuit used for the EIS data analysis.

The pH of the supporting electrolyte also plays a major role in the electrochemical behaviour of glucose. A linear relationship was obtained between the anode potential (E_{pa}) and pH, suggesting the participation of protons during the electrochemical process (Fig. 8(B)). The anode potential shifted to more negative values as the pH increased. The obtained slope of 0.056 V pH^{-1} was close to the Nernstian slope of 0.059 V pH^{-1} for a reversible two-proton/two-electron process at room temperature.[47]

In this study, the optimal potential for amperometric detection at the electrode in the potential range of 0.3 to 0.6 V was investigated. As shown in Fig. 9, the anodic current response increases rapidly from 0.3 to 0.55 V, and when the applied potential further increases to +0.6 V, the amperometric current of glucose decreases. Maximum sensitivity occurred at an operating potential of 0.55 V (*vs.* Ag/AgCl). Thus, 0.55 V was chosen as the working potential in the subsequent experiments. This potential value is more negative compared with previous studies (Table 1) and the lower detection potential significantly diminished the influence of the easily oxidized species.[9]

3.6. Amperometric detection of glucose

In this work, a single potential time base (TB) amperometric method was performed for the oxidation of glucose. It is a sensitive and reliable technique to evaluate the electroactivities of the catalysts applicable for the electrochemical glucose sensors in low concentrations of analytes.[48] Because this method can help achieve the effective mixing of a sample solution and convective mass transport to the electrode surface and results in rapid detection of an analyte.[17]

The electrocatalytic oxidation of glucose at ZnO/Co_3O_4/rGO was studied using TB amperometry by the successive addition of glucose standard under a continuous stirring of 10 mL of 0.1 M NaOH. Fig. 10A shows the amperometric responses at 0.55 V of ZnO/Co_3O_4/rGO/GCE electrode with a subsequent increase in glucose concentration from 0.0001 to 10 mM; the steady state current reached a fast response time of 3 s, owing to the excellent electrocatalytic activity. With the further addition of glucose in each step with a sample interval of 80 s, the current response increased and a steady state current response was attained.

The relationship between the electrocatalytic current and glucose at different concentrations at the ZnO/Co_3O_4/rGO/GCE is shown in Fig. 10(B); demonstrating a good linear relationship in the range of 0.015–10 mM. The corresponding linear fit equation is obtained as I (μA) = 108.59246 (mM) + 57.6544 with the correlation coefficient (R^2) 0.99065 and slope 108.59246 μA mM^{-1}. According to Anitha *et al.*,[11] the sensitivity in μA mM^{-1} cm^{-2} can be calculated by the slope of the calibration graph divided by the surface area of the working electrode. The LOD and sensitivity for glucose determination were obtained as 0.043 μM and 1551.38 μA mM^{-1} cm^{-2}, respectively. The limit of detection (LOD) of the amperometric glucose sensor was estimated using the equation; $3S_b/m$, where S_b is the standard deviation-obtained measurements of the signal and m is the slope value that was taken from the calibration plot.

A comparison of the analytical performance of ZnO/Co_3O_4/rGO/GCE with other recently reported non-enzymatic glucose sensors from the literature is shown in Table 3. Obviously, the performance of this ZnO/Co_3O_4/rGO/GCE sensor is nearly

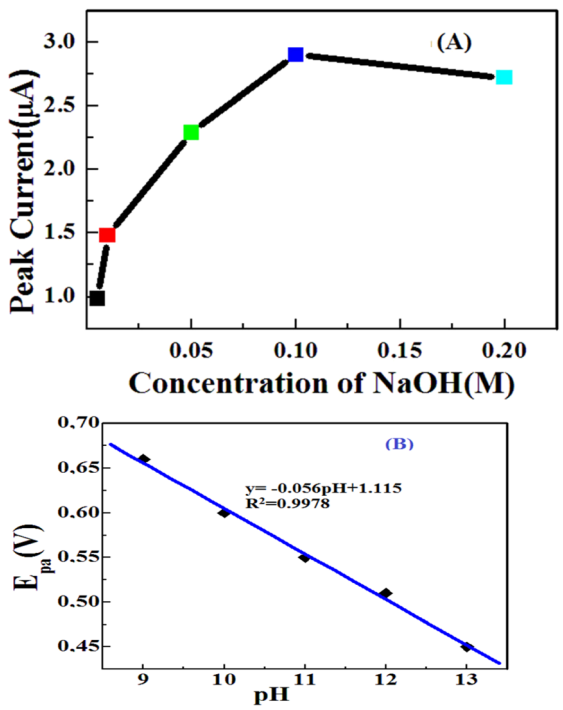

Fig. 8 (A) The plot of anodic current of ZnO/Co_3O_4/GCE *versus* different concentrations of NaOH (0.005 M up to 0.2 M) upon the addition of 2 mM glucose at a scan rate of 50 mV s^{-1}. (B) The plot of anode potential (E_{pa}) *vs.* pH values NaOH.

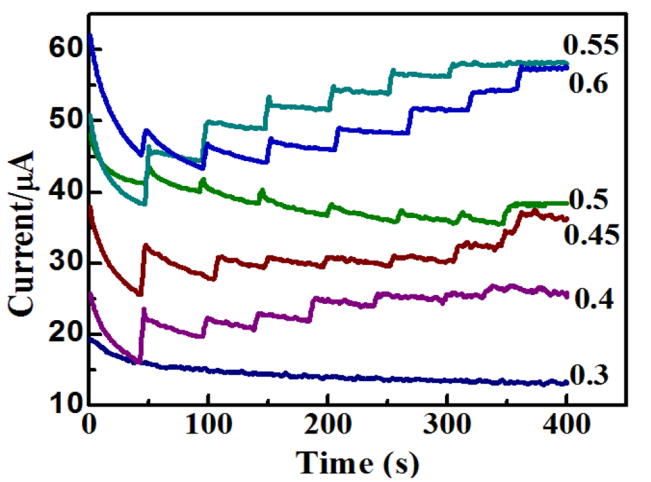

Fig. 9 Amperometric *i*–*t* graphs of ZnO/Co_3O_4/rGO/GCE to the successive injections of 2 mM glucose at different applied potentials from 0.3 V up to 0.6 V.

Table 1 Comparison of the analytical performance of the ZnO/Co_3O_4/rGO sensor with other recently published non-enzymatic glucose sensors

Sensor	E (V)	Sensitivity (μA mM^{-1} cm^{-2})	Liner range (mM)	LOD (μM)	Ref.
Cu_2O/rGO	0.55	1145.3	101 μM–0.1 mM	—	49
Co_3O_4/rGO	0.55	1366	0.0005–1.277 mM	0.18 μM	6
Co_3O_4/NiO	0.5	2477	1 μM–9.055 mM	0.17 μM	18
NiO/CuO/rGO	0.5	1046	5 μM–4.85 mM	0.5 μM	19
NiO/Au/PANI/rGO	0.55	—	0.09–6 mM	0.23 μM	20
ZnO/GCE	0.68	631.3	1–8.6 mM	0.043 μM	50
ZnO/rGO	—	39.78	0 to 33.5 μM	0.2 μM	51
Co–CoO–Co_3O_4	0.55	949.3	0.005–0.6 mM	0.92 μM	52
ZnO/CuO	—	1457.5	0.1 to 4167 μM	0.038 μM	17
TiO_2/Co_3O_4	0.5	2008.82	0.2–3.0 mM	0.3396 μM	43
Pt/Ni@rGO	0.5	106.5	0.02–5.0 mM	6.3 μM	53
ZnO@rGO		481	2×10^{-5}–7.2×10^{-3} mM	0.008 μM	54
ZnO/Co_3O_4/rGO	0.55	1551.38	0.015–10 mM	0.043 μM	This work

comparable to that of other zinc and cobalt-based non-enzymatic glucose sensors in view of low detection potential, high sensitivities, wide linear range, and low LOD.

3.7. Effect of interferences on analytical response

Assessing the selectivity of the current sensor for large sample matrices was crucial and should be studied. Therefore, an investigation was performed on the probable effects of some naturally occurring interfering substances such as uric acid, ascorbic acid, and other food supplement carbohydrate compounds, which usually co-exist with glucose in human blood or other real samples. Here, the interference test regarding 0.1 mM interfering species with 1 mM glucose was performed to investigate the selectivity based on the ZnO/Co_3O_4/rGO/GCE electrode in 0.1 M NaOH at an applied potential of 0.55 V. As shown in Fig. 11A, the sensor response showed no obvious amperometric signal towards ascorbic acid and uric acid and showed excellent selectivity toward common interfering species. It can be seen that no significant signals were observed for the tested interfering species, just a short time after their addition; whereas, the well-defined glucose oxidation currents were obtained before and after the addition of the interfering species. The effects of glucose-similar compounds (maltose, fructose, and sucrose) have a small response on the amperometric signals at 0.55 V of the applied potential. But the result of glucose was several times higher than those for fructose, lactose, and sucrose, which indicated that the influence may not be severed. Therefore, this ZnO/Co_3O_4/rGO nanocomposite electrode provided good selectivity for the amperometric determination of glucose with high potential applications in clinical diagnostic and also food industries.

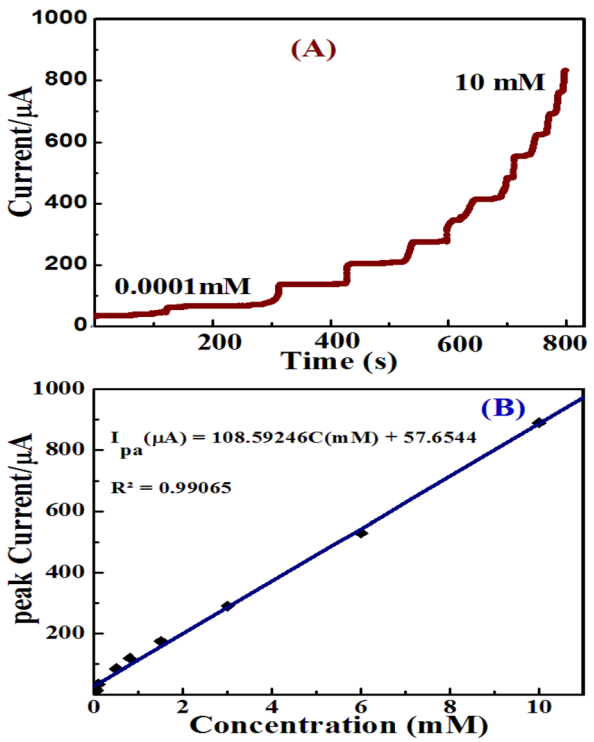

Fig. 10 (A) A typical amperometric *i–t* curve of ZnO/Co_3O_4/rGO electrode to successive addition of glucose solution into a stirred system of 0.1 M NaOH (pH 13.0) at +0.55 V. Rotating speed 3000 rpm. (B) Linear calibration plot of the corresponding current *versus* the glucose concentration.

Another challenge for non-enzymatic sensors based on metals, metal oxides, or metal alloys is that they are prone to poisoning by chloride ions and thus lose their catalytic activity.[45] To check the stability and reliability of the ZnO/Co_3O_4/rGO/GCE as glucose sensors, they were examined for the amperometric response in a solution comprising 0.05 M NaCl and 0.1 M NaOH, to mimic physiological conditions; there was no obvious current decrease due to chloride poisoning. The CV curves of ZnO/Co_3O_4/rGO/GCE (Fig. 11B) obtained in 0.1 M NaOH containing 2 mM glucose with and without 0.05 M NaCl at 0.55 V working potential were almost identical. The results indicated that the proposed sensor was unaffected by chloride ions and could be used in the presence of chloride ions.

3.8. Stability, reproducibility, and repeatability of the ZnO/Co_3O_4/rGO modified sensor

The stability, repeatability, and reproducibility of the resulting sensor were also investigated in this work. The

Table 2 Working condition and Amperometric determination of glucose spiked in human urine samples (n = 3)

Glucose concentration of originalurine sample	Glucose added (mM)	Glucose detected[a] (mM)	RSD[b] (%)	Recovery (%)
5.4 mg dL^{-1} (0.30 mM)[c]	0.0	0.315 ± 0.025	4.875081	—
	2.0	2.29 ± 0.06	2.620087	99.5
	3.0	3.31 ± 0.056	1.682104	100.3
	5.0	5.22 ± 0.10	1.917674	98.46

[a] Standard addition method. [b] Relative standard deviation of three measurements. [c] Measured by commercial spectrophotometer.

Table 3 The practical application of ZnO/Co_3O_4/rGO sensor in the food industry (n = 3)

Food samples	Glucose content (labelled value)	This sensor (mM)	Relative difference (mM)
Milk	2 mM	2.85 ± 0.198	+0.85
Fruit juice	0.1 mM	0.114 ± 0.065	+0.014

sensor was stored at room temperature for 8 days and its sensitivity was tested every 2 days. It was found that the sensor retained about 83% of its initial response after 8 days of storage; suggesting good stability of the ZnO/Co_3O_4/rGO/GCE glucose sensor (Fig. 12). To estimate the repeatability of the proposed method, the RSD of the four successive measurements of the peak current of 2 mM glucose on ZnO/Co_3O_4/rGO/GCE-modified electrode was calculated to be 2.9%, which demonstrated good repeatability of the method. The electrode-to-electrode reproducibility of ZnO/Co_3O_4/rGO/GCE was investigated by comparing the amperometric current response to glucose at four modified electrodes. All four electrodes were fabricated with 8 μL of ZnO/Co_3O_4/rGO nanocomposite (5 mg mL^{-1}) suspension by the drop coating method and then dried in an air oven. Then, all the electrodes were individually tested in the presence of 2 mM of glucose in 0.1 M NaOH. The relative standard deviation (RSD) obtained was found to be 3.26%, thus indicating an acceptable reproducibility of the present nanocomposite-modified electrode.

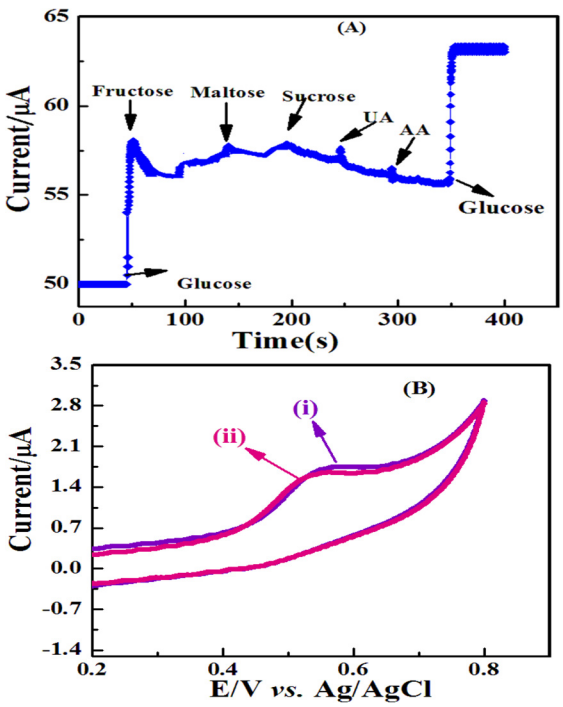

Fig. 11 (A) Amperometric response of the ZnO/Co_3O_4/rGO/GCE in 0.1 M NaOH (pH 13) upon the successive addition of glucose (1 mM), fructose (0.1 mM), maltose (0.1 mM), sucrose (0.1 mM), UA (0.1 mM), AA (0.1 mM), and 1 mM glucose, respectively, (B) CVs of a ZnO/Co_3O_4/rGO/GCE containing 1 mM glucose and 0.1 M NaOH solution (curve i) and in the presence of 0.05 M NaCl (curve ii) at a scan rate of 50 mV s^{-1}.

3.9. Determination of glucose in real samples

The ZnO/Co_3O_4/rGO composite-modified GCE was used to investigate the real-time analysis of glucose in urine samples of healthy humans; the sample was obtained from the Hiwot Fana specialized university hospital, Harar town, Ethiopia, and tested using amperometry at the applied potential of 0.55 V. The concentration of the glucose level in the collected human urine samples was also measured using a commercial spectrophotometer, which measured about 5.4 ± 0.0625 mg dL^{-1} (0.30 mM) using three replicate measurements. Furthermore, a known concentration of urine samples was diluted 100 times with 0.1 M NaOH solution and then used for the real sample analysis.[55] The amperometric i–t method was performed before and after the addition of glucose in the urine sample at the applied potential of 0.55 V. The determination of the glucose was performed with the diluted sample, while the recovery analyses of the standards (2, 3, and 5 mM) from solutions of the standard glucose and the diluted human urine sample were within the linear working range (Fig. 13). To determine the accuracy of the results, three measurements were performed on each sample. Table 2 shows the comparison of the proposed sensor-determined values, the commercial spectrophotometer measurement, and the spiked values. The resulting glucose concentrations estimated from the calibration curves using this modified

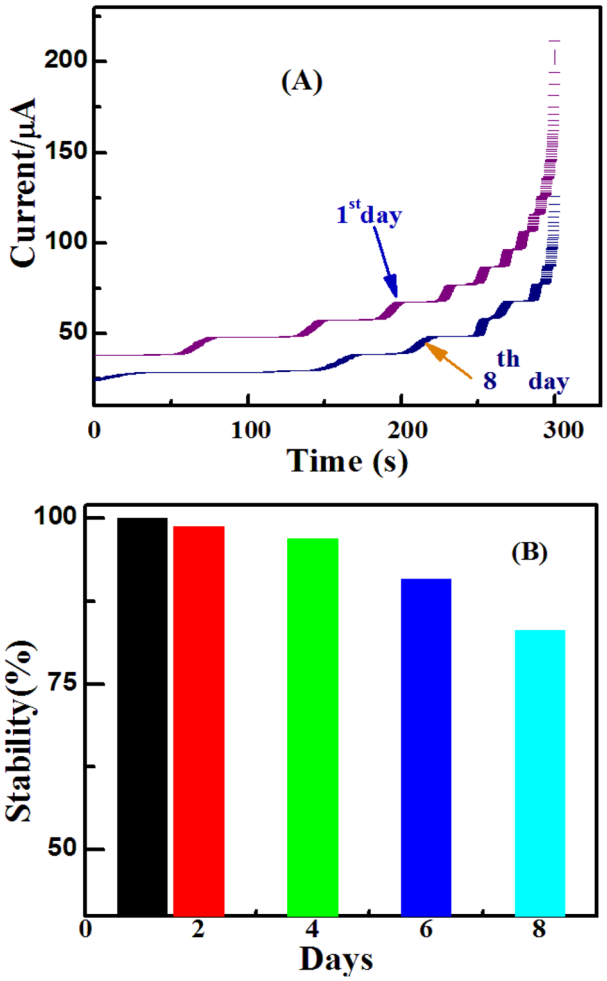

Fig. 12 (A) The first-day and eighth-day amperometric responses of the ZnO/Co_3O_4/rGO/GCE in 0.1 M NaOH upon the successive addition of 2 mM glucose at 0.55 V, (B) the percent stability of the ZnO/Co_3O_4/rGO nanocomposite sensor for eight days.

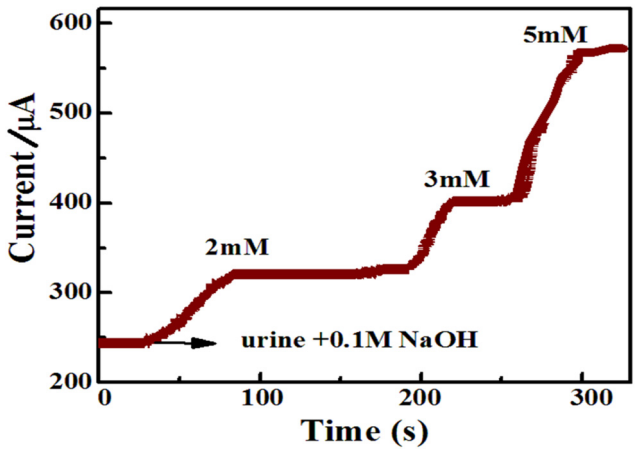

Fig. 13 Amperometric *i–t* response of ZnO/Co_3O_4/rGO/GCE for successful injection of the standard glucose solution (2, 3, and 5 mM) at an applied potential of 0.55 V, with a rotation speed of 1000 rpm.

electrode were similar to those achieved using a spectrophotometric method in a medical diagnostic laboratory and had only a 1.15% difference, as clearly shown in Table 2. Analytical recoveries of the added glucose into the urine samples were from 98.46% to 100.3%, which indicated that the fabricated electrode, ZnO/Co_3O_4/rGO/GCE is a very suitable modified electrode for the detection of glucose for practical real sample analysis.

Moreover, the practical application of the developed sensor in the food industry can be tested by the determination of glucose in fruit juice and milk samples using amperometry. For this purpose, commercially available mango fruit juice and milk samples were used, which were purchased from a local supermarket in Harar Town, Ethiopia. The dissolved milk was prepared based on the instructions of the manufacturer for drinking purposes. Then, the fruit juice and milk solution were centrifugated at 3000 rpm for 15 min and the obtained clear sample was analyzed. The samples were diluted appropriately (1 mM and 2 mM) using deionized water prior to the analysis to ensure that the glucose concentrations were within the linear working range and to reduce possible matrix effects.[39] Then, 5.0 ml of the clear fruit juice was diluted with 20.0 ml of the 0.1 M NaOH solution as a supporting electrolyte in order to obtain the final real samples.[24,56] In the amperometric responses for the successive addition of the final real sample, a fast and remarkable increase occurred in the current, indicating that the sensor has a rapid and sensitive response to changes in glucose concentration. This shows the good electrocatalytic capability of ZnO/Co_3O_4/rGO/GCE and its applicability in the determination of glucose in real samples in the food industry. The electrochemical detection of glucose in fruit juice agreed with the manufacturer values (Table 3), however, the detection of glucose in the milk sample interfered with different matrices at 0.55 V working potential and the result showed somewhat increased values compared with those provided by the manufacturer, and this was because of the detection of other interferences on the electrode surface (Fig. 14). This problem may be improved using lower working applied potential or by diluting the real samples at a higher dilution factor.

Conclusion

In this study, we investigated a more sensitive and selective ZnO/Co_3O_4/rGO nanocomposite for non-enzymatic electrochemical glucose sensing and used the sensor for the detection of glucose in the human urine sample and some selected samples from food industries. For this purpose, ZnO/Co_3O_4/rGO nanocomposite sensor was synthesized by a simple hydrothermal growth mechanism of ZnO and Co_3O_4 nanostructures on reduced graphene oxide. The ZnO/Co_3O_4/rGO nanocomposite sensor exhibited outstanding electrochemical performance with high catalytic activity for glucose oxidation. This is due to a large surface area and higher conductivity of rGO. Compared with other previous reports, the ZnO/Co_3O_4/rGO nanocomposite sensor showed good stability, excellent selectivity, good sensitivity, and reproducibility, higher sensitivity (1551.38 μA mM^{-1} cm^{-2}), a

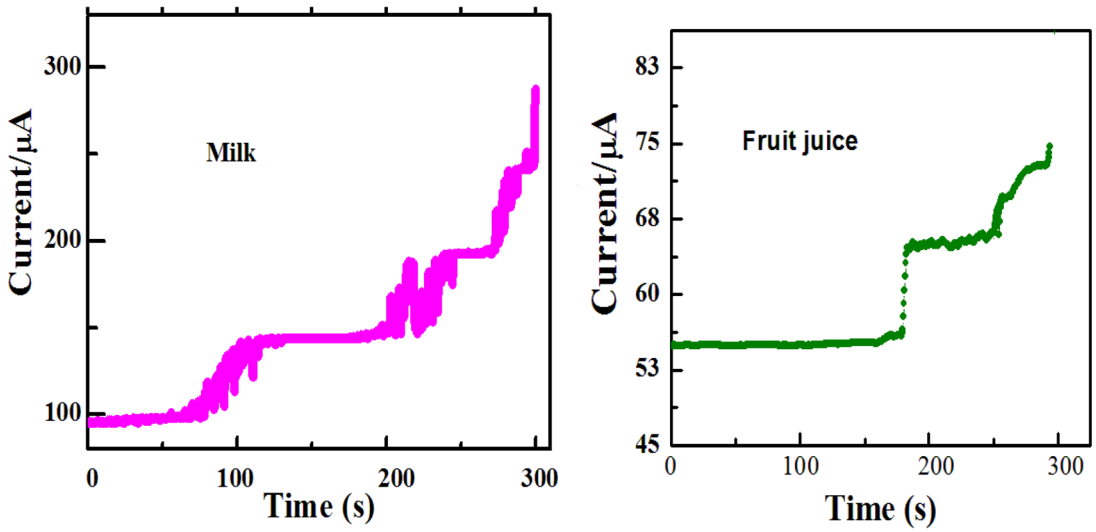

Fig. 14 Amperometric responses of ZnO/Co_3O_4/rGO/GCE towards two different real samples (milk and fruit juice) in 0.1 M NaOH at an applied potential of 0.55 V.

lower detection limit of 0.043 μM (S/N = 3) and broad linear range (0.015–10 mM) without any polymeric binder (Nafion) for the attachment of the nanocomposite on the GC surface. The practical application of the proposed sensor positively agreed with the spectrophotometric method used in hospitals and the glucose label value provided by the food industry.

Author contributions

This work was completed through the contributions of all authors. BAH and AAT conducted the laboratory work; analysis and interpretation of the results. GS and AMT read and edited the manuscript. All the authors have read and approved the final manuscript.

Conflicts of interest

There are no conflicts to declare.

Acknowledgements

We thank Hiwot Fana specialized hospital, Harar Town, Ethiopia for providing urine samples and the Ministry of Education, the Federal Democratic Republic of Ethiopia for financial support.

References

1 E. Reitz, W. Jia, M. Gentile, Y. Wang and Y. Lei, CuO Nanospheres Based Nonenzymatic Glucose Sensor, *Electroanalysis*, 2008, **20**, 2482–2486.
2 Z. Zhu, L. G. Gancedo, A. J. Flewitt, H. Xie, F. Moussy and W. I. Milne, A Critical Review of Glucose Biosensors Based on Carbon Nanomaterials: Carbon Nanotubes and Graphene, *Sensors*, 2012, **12**, 5996–6022.
3 J. Wang, Electrochemical Glucose Biosensors, *Chem. Rev.*, 2008, **108**, 814–825.
4 C. Wang and A.-R. Lee, Recent Developments in Blood Glucose Sensors, *J. Food Drug Anal.*, 2015, **23**, 191–200.
5 M. M. Rahman, A. Saleh, J. Joon, S. J. Ahn and L. Jae-Joon, AComprehensive review of Glucose Biosensor based on Nanostructured Metal-Oxides, *Sensors*, 2010, **10**, 4855–4886.
6 Z. Yaolin, L. Ping, L. Hongbo and C. Shouhui, Controllable Growth of Cobalt Oxide Nanoparticles on Reduced Graphene Oxide and its Application for Highly Sensitive Glucose Sensor, *Int. J. Electrochem. Sci.*, 2014, **9**, 7369–7381.
7 N. S. Sachindra, N. Shinji and N. S. Surendra, ZnO Nanorod Based Non-Enzymatic Optical Glucose Biosensor, *J. Biomed. Nanotechnol.*, 2015, **11**, 988–996.
8 X. Qin, Z. Yu, J. Z. Xu and Z. Jun-Jie, Preparation of Functionalized Copper Nanoparticles and Fabrication of a Glucose Sensor, *Sens. Actuators, B*, 2006, **114**, 379–386.
9 K. E. Toghill and R. G. Compton, Electrochemical Non-enzymatic Glucose Sensors: A Perspective and an Evaluation, *Int. J. Electrochem. Sci.*, 2010, **5**, 1246–1301.
10 R. Tipawan, P. Eakkasit, A. Jaclyn, H. Charles and C. Orawon, Development of Electrochemical Paper-based Glucose Sensor using cellulose-4-aminophenylboric acid modified screen printed electrode, *Electroanalysis*, 2016, **28**, 462–468.
11 V. Anitha, T. E. Kumary, J. D. Mary Nancy and K. Sreevalsan, Nonenzymatic Glucose Sensor: Glassy Carbon Electrode Modified with Graphene-Nickel/Nickel Oxide Composite, *Int. J. Electrochem. Sci.*, 2013, **8**, 2220–2228.
12 K. Tian, P. Megan and T. Ashutosh, A Review of Recent Advances in Nonenzymatic Glucose Sensors, *Mater. Sci. Eng. C*, 2014, **41**, 100–118.
13 M. Pastaa, L. M. Fabio and Y. Cuib, Mechanism of Glucose Electrochemical Oxidation on Gold Surface, *Electrochim. Acta*, 2010, **55**, 5561–5568.
14 H. Yao, Z. Xiaoying, Z. Daojun, L. Lin and Y. Baiqing, Shape controlled synthesis of Cu_2O Microstructures at Glassy Carbon Electrode by Electro-chemical Method for Non-

enzymatic Glucose Sensor, *Int. J. Electrochem. Sci.*, 2013, **8**, 12184–12191.

15 L. Yancai, H. Fuying, C. Jie, M. Tao, L. Shunxing, W. Fei, F. Shuqing and L. Yuanjun, A High Performance Enzyme-Free Glucose Sensor Based on the Graphene-CuO Nanocomposites, *Int. J. Electrochem. Sci.*, 2013, **8**, 6332–6342.

16 J. Chen, W. Zhang and J. Ye, Nonenzymatic Electrochemical Glucose Sensor Based on MnO_2/MWNTs Nanocomposite, *Electrochem. Commun.*, 2008, **10**, 1268–1271.

17 H. Karuppiah, V. N. Murugan, C. Shen-Ming, H. Shin, M. Tsai Bih-Show Lou, A. Ajmal and M. A. Fahad, A simple Hydrothermal Synthesis and Fabrication of Zinc Oxide–Copper oxide heterostructure for the sensitive determination of nonenzymatic glucose biosensor, *Sens. Actuators, B*, 2015, **221**, 1299–1306.

18 R. Ramasamy, K. Ramachandran, G. P. Geo, R. Rasu, A. T. Helen and K. G. Gnana, Design and development of Co_3O_4/NiO composite nanofibers for the application of highly sensitive and selective non-enzymatic glucose sensors, *RSC Adv.*, 2015, **5**, 76538–76547.

19 S. J. Li, X. Yun, L. H. Lin, Q. F. Zhu, Y. Tian and J. M. Du, Facile Synthesis of NiO/CuO/reduced Graphene Oxide Nanocomposites for Use in Enzyme-free Glucose Sensing, *Int. J. Electrochem. Sci.*, 2016, **11**, 6747–6760.

20 K. Ghanbari and F. Ahmadi, NiO hedgehog-like nanostructures/Au/polyaniline nanofibers/reduced graphene oxide nanocomposite with electrocatalytic activity for non-enzymatic detection of glucose, *Anal. Biochem.*, 2017, **518**, 143–153.

21 J. A. Rodriguez, T. Jirsak, J. Dvorak, S. Sambasivan and D. Fischer, Reaction of NO2 with Zn and ZnO: Photoemission, XANES, and Density Functional Studies on the Formation of NO3, *J. Phys. Chem. B*, 2000, **104**, 319–328.

22 Y. Sun, S. Zichao, X. Shuli, M. Li, X. Chunhui, D. Shujiang, F. Li and G. Guoxin, Ultrafine Co-doped ZnO nanoparticles on Reduced graphene oxide as an Efficient electrocatalyst for oxygen reduction reaction, *Electrochim. Acta*, 2017, **224**, 561–570.

23 S. Kumar and B. Sukumar, Graphene-Oxide Nano Composites for Chemical Sensor Applications, *C*, 2016, **2**, 12–20.

24 X. Zhang, L.-x. Ma and Y.-C. Zhang, One-pot facile fabrication of graphene-Zinc oxide composite and its enhanced sensitivity for simultaneous electrochemical detection of ascorbic acid, dopamine and uric acid, *Sens. Actuators, B*, 2016, **227**, 488–496.

25 L. Zhu, S. Zhang, Y. Cui, H. Song and X. Chen, One step synthesis and capacitive performance of graphene nanosheets=Mn_3O_4 composite, *Electrochim. Acta*, 2013, **89**, 18–23.

26 A. M. Golsheikh, N. M. Huang, H. N. Lim, C. H. Chia, I. Harrison and M. R. Muhamad, One-pot hydro-thermal synthesis and characterization of FeS2(pyrite)=graphene nanocomposites, *Chem. Eng. J.*, 2013, **218**, 276–284.

27 X. M. Chen, G. H. Wu, Y. Q. Jiang and Y. R. C. Wang, Graphene and graphene-based nanomaterials: The promising materials for bright future of electroanalytical chemistry, *Analyst*, 2011, **136**, 4631–4640.

28 L. Luo, L. Zhu and Z. Wang, Nonenzymatic amperometric determination of glucose byCuO nanocubes-graphene nanocomposites modified electrode, *Bioelectrochemistry*, 2012, **88**, 156–163.

29 K. Agilandeswari and A. R. Kumar, Synthesis, Characterization and Optical properties of Co_3O_4 by Precipitation method, *Int. J. ChemTech Res.*, 2014, **6**, 2089–2092.

30 N. A. Salahuddin, E. Maged and M. I. Ebtisam, Synthesis and Characterization of ZnO Nanoparticles via Precipitation Method: Effect of Annealing Temperature on Particle Size, *Nanosci. Nanotechnol.*, 2015, **5**, 82–88.

31 P. K. Labhane, L. B. Patle, V. R. Huse, G. H. Sonawane and S. H. Sonawane, Synthesis of reduced graphene oxide sheets decorated by zinc oxide nanoparticles: Crystallographic, optical, and morphological and photocatalytic study, *Chem. Phys. Lett.*, 2016, **661**, 13–19.

32 D. Liang, C. Can, H. Hu, W. Yaping, S. Xu, Y. Beili, P. Li, L. Bingqing and S. Honglei, One-step hydrothermal synthesis of anatase TiO2/reduced graphene oxide nanocomposites with enhanced photocatalytic activity, *J. Alloys Compd.*, 2014, **582**, 236–240.

33 Y. Zhu, S. Murali, W. Cai, X. Li, J. W. Suk, J. R. Potts and R. S. Ruoff, Graphene and graphene oxide: synthesis, properties, and applications, *Adv. Mater.*, 2010, **22**, 3906–3924.

34 T. K. Jana, A. Pal and K. Chatterjee, Magnetic and photocatalytic study of Co3O4/ZnO nanocomposite, *J. Alloys Compd.*, 2015, **653**, 338–344.

35 F. Ahmed, K. Shalendr, A. M. S. Nishat, S. Y. Anwar, K. Lee, P. Gyung-Suk, H. K. B. Dae-Won and G. L. Chan, Preparation and characterizations of polyaniline (PANI)/ZnO nanocomposites film using solution casting method, *Thin Solid Films*, 2011, **519**, 8375–8378.

36 A. P. Sharma and S. Kumar, Synthesis and Characterization of NiO-ZnO Nano Composite, *Nano Vision*, 2011, **1**, 115–122.

37 S. Shahabuddin, M. S. Norazilawati, H. I. Fatem, M. S. Muhammad and M. H. Nay, Synthesis of chitosan grafted-polyaniline/Co_3O_4 nanocube nanocomposites and their photocatalytic activity toward methylene blue dye degradation, *RSC Adv.*, 2015, **5**, 83857–83867.

38 R. Karthik and S. Thambidurai, Synthesis of cobalt doped ZnO/reduced graphene oxide nanorods as active material for heavy metal ions sensor and antibacterial activity, *J. Alloys Compd.*, 2017, **715**, 254–265.

39 N. Nontawong, A. Maliwan, J. Purim, T. Suparb and C. Sanoe, Non-Enzymatic Glucose Sensors for Sensitive Amperometric Detection Based on Simple Method of Nickel Nanoparticles Decorated on Magnetite Carbon Nanotubes Modified Glassy Carbon Electrode, *Int. J. Electrochem. Sci.*, 2017, **12**, 1362–1376.

40 L. Wang, J. Fu, H. Hou and Y. Song, A Facile Strategy to Prepare Cu_2O/Cu Electrode as a Sensitive Enzyme-free

Glucose Sensor, *Int. J. Electrochem. Sci.*, 2012, **7**, 12587–12600.

41 Y. Ding, Y. Wang, L. Su, M. Bellagamba, H. Zhang and Y. Lei, Electrospun Co_3O_4 nanofibers for sensitive and selective glucose detection, *Biosens. Bioelectron.*, 2010, **26**, 542–548.

42 L. Mian, H. Ce, Z. Yufan, X. Bo and G. Liping, Facile synthesis of ultrafine Co_3O_4 nanocrystals embedded carbon matrices with specific skeletal structures as efficient non-enzymatic glucose sensors, *Anal. Chim. Acta*, 2015, **861**, 25–35.

43 Z. Gao, Z. Liqiang, C. Ma, Q. Zhou, Y. Tang, Z. Tu, W. Yang, L. Cui and Y. Li, TiO_2 decorated Co_3O_4 acicular nanotube arrays and its application as a non-enzymatic glucose sensor, *Biosens. Bioelectron.*, 2016, **80**, 511–518.

44 G. Chunyan, Z. Xuan, H. Huanhuan, X. Cailing and X. Han, Co3O4 microspheres with free-standing nanofibers for high performance non-enzymatic glucose sensor, *Analyst*, 2013, **138**, 6727–6731.

45 F. J. Garcia, P. Salazar, F. Yubero and A. R. González-Elipe, Non-enzymatic Glucose electrochemical sensor made of porous NiO thin films prepared by reactive magnetron sputtering at oblique angles, *Electrochim. Acta*, 2016, **201**, 38–44.

46 T. Alizadeh and M. Shabnam, A Nafion-free non-enzymatic amperometric glucose sensor based on copper oxide nanoparticles–graphene nanocomposite, *Sens. Actuators, B*, 2014, **198**, 438–447.

47 R. Vasiliadou, M. M. N. Esfahani, J. B. Nathan and J. W. Kevin, A Disposable Microfluidic Device with a Screen Printed Electrode for Mimicking Phase II Metabolism, *Sensors*, 2016, **16**, 1418–1433.

48 B. Halima, S. A. Mohammad and J. Seungwon, Ultra-fast and highly sensitive enzyme-free glucose biosensing on a nickel–nickel oxide core–shell electrode, *RSC Adv.*, 2017, **7**, 3554–3562.

49 X. Feng, G. L. Changfa, J. Ning and Y. Hu, Facile Growth of Cu_2O Nanowires on Reduced Graphene Sheets with High Nonenzymatic Electrocatalytic Activity toward Glucose, *J. Am. Ceram. Soc.*, 2014, **97**, 811–815.

50 T. Dayakar, K. Venkateswara Rao, K. Bikshalu, V. Rajendar and S.-H. Park, Novel synthesis and structural analysis of zinc oxide nanoparticles for the non enzymatic glucose biosensor, *Mater. Sci. Eng., C*, 2017, **75**, 1472–1479.

51 S. M. S. Dhanush, F. Rossignol and H. S. Nagaraja, Microwave assisted synthesis of rGO/ZnO composites for non-enzymatic glucose sensing and supercapacitor applications, *Ceram. Int.*, 2017, **43**, 4895–4903.

52 J. Yu, Y. Ni and M. Zhai, Highly selective non-enzyme glucose detection based on Co-CoO-Co_3O_4 nanocomposites prepared via a solution-combustion and subsequent heat-treating route, *J. Alloys Compd.*, 2017, **723**, 904–911.

53 R. Ayranci, B. Demirkan, B. Sen, A. Şavk, M. Ak and F. Şen, Use of the Monodisperse Pt/Ni@rGO Nanocomposite Synthesized by Ultrasonic Hydroxide Assisted Reduction/Method in Electrochemical Nonenzymatic Glucose Detection, *Mater. Sci. Eng., C*, 2019, **99**, 951–956.

54 K. B. Babitha, P. S. Soorya, A. Peer Mohamed, R. B. Rakhi and S. Ananthakumar, Development of ZnO@rGO nanocomposites for the enzyme free electrochemical detection of urea and glucose, *Mater. Adv.*, 2020, **1**, 1939–1951.

55 S. Samuei, F. Jila, R. Zolfaghar, A. Shomali and H. Biuck, Synthesis and characterization of graphene quantum dots/CoNiAllayered double-hydroxide nanocomposite application as a glucose sensor, *Anal. Biochem.*, 2017, **521**, 31–39.

56 S. Ashok Kumar, H.-W. Cheng, S.-M. Chen and S.-F. Wang, Preparation and Characterization of Copper Nanoparticles/Zinc Oxide Composite Modified Electrode and its application to glucose sensing, *Mater. Sci. Eng. C*, 2010, **30**, 86–91.